Creep Crack Growth in an Austenitic Stainless Steel Welded Joint

H. SASSOULAS and P. BALLADON
Unirec, Groupe Usinor-Sacilor, BP 50, 42702 Firminy Cédex, France

The study of the behaviour of materials under fatigue and creep condition is made necessary by the development of structures submitted to high temperatures, such as may be encoutered in the nuclear, aeronautical, oil or chemical industries. During their service life, these structures are submitted to start-up and shut-down cycles, and are maintained for long periods at high temperatures, which may lead to their rupture by a combination of fatigue and creep damage. In the case of fatigue, crack growth rate da/dN can be correlated to a mechanical parameter such as ΔK, by using Paris law. As far as creep is concerned, up to now no correlation has been found between crack growth rate and a mechanical parameter. Cracks usually grow from pre-existing flaws ; welded joints are particularly prone to the presence of these flaws. It is therefore the aim of this work to study the evolution under creep conditions of such flaws in a welded joint representative of the internal body of the liquid metal fast breeder reactor Superphenix. The studied steel is a 316 L type austenitic stainless steel, developped within the Superphenix project for its good creep properties at the reactor working temperature : 550°C. The filler metal has also been chosen to obtain creep resistant welded joints and meets Superphenix specifications. By creating an artificial defect in the sample, we wish to study the initiation and propagation of a crack under creep conditions. Several positions of the initial defect with respect to the welded joints have been tried in order to determine whether any was more dangerous. Different sample geometries have also been tried in order to assess their influence. The obtained results have been compared to those already available concerning base metal, within a global fracture mechanics approach, and also by microscopic damage observations.

EXPERIMENTS

Material

All base metal comes from a heat processed in 25 mm thick plates. Its chemical composition is given below :

C	Mn	Si	S	P	Ni	Cr	Mo	Cu	Al	Co
0.02	1.72	0.315	0.002	0.023	11.65	17.32	2.27	0.125	0.005	0.200

Four welded joints were used for specimen cutting. All joints were made using the manual metal arc technic according to Superphenix fabrication specifications.

Three of them (later refered to as type I) were made with the same batch of electrodes, resulting in the chemical composition indicated below. A K chamfer was machined prior to welding.

Weld metal chemical composition

C	Mn	Si	S	P	Ni	Cr	Mo	Cu	Al	Co	V
0.047	1.5	0.52	0.013	0.018	11.65	18.38	1.92	0.045	0.005	0.058	0.070

The fourth (later refered to as type II) was made with another batch of electrodes resulting in the chemical composition given below. An X chamfer was machined prior to welding.

C	Mn	Si	S	P	Ni	Cr	Mo	Cu	Co	N2 (*)
0.043	1.59	0.6	0.011	0.017	11.67	18.42	1.94	0.06	0.11	0.033

(*) analysis performed on electrode

The weld metal has a duplex structure, with about 5 % ferrite.

Specimens

The tests were carried out on compact tension specimens and notched axisymetric specimens. Eleven CT 40-10 specimens (W = 80 mm, B = 10 mm) were machined from the type I joints. Two compact tension specimens CT 20 (W = 40 mm, B = 20 mm) and one notched axisymteric specimen FLE 0.05 were machined from the type II joint (the FLE 0.05 specimen geometry is given in figure 1). For the CT 40-10 specimens, six flaw positions were tested :
- Positions 1, 2, 3 : flaw parallel to the welded joint ; in the heat affected zone, along the fusion line, and at the center of the weld metal (respectively)
- Positions 4, 5, 6 : initial flaw perpendicular to the welded joint with the notch extremity respectively in the HAZ, on the fusion line or at the center of the weld.

The initial flaw was machined by thread electroerosion : the notch extremity radius being 75 µm.

The six positions are shown below :

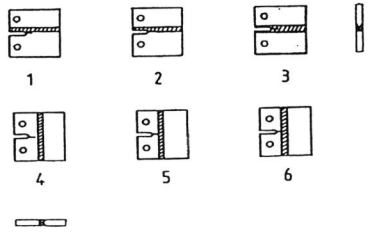

The two CT 20 specimens had an initial fatigue flaw parallel to the welded joint, at the center of it. One of them was side-grooved resulting in an equivalent thickness of $B_N \leq 16$ mm (20 % SG). The welded joint was perpendicular to the axis of the FLE 0.05 specimen, with the notch machined in the weld metal.

In order to understand the influence of sample geometry, it is necessary to point out the following facts :
- in a CT 40-10 specimen, the amount of weld metal represents roughly 7 % of the total specimen
- in a CT 20 specimen, the weld metal represents roughly 25 % of the specimen
- in the FLE 0.05 specimen, the zone where creep deformation occurs is situated almost entirely in the weld metal.

Testing procedures

Creep crack growth was carried out under a constant load. The following measurements were made on the specimens : Displacement Δ along the load line was measured by an extensometer, Crack length was measured by applying a constant intensity of 9A to the specimen and recording the potential between two points on each side of the crack. The initiation time ti is conventionnally taken as the time when crack length measured by the above mentionned technic is found equal to 100 µm.

Testing temperatures were 600°C and 650°C. Initial crack length a/W was equal to 0.35 for CT 40-10 specimens, 0.486 for the plain CT 20 and 0.586 for the side groowed CT 20. The load varied from 13720 N to 22130 N for CT 40-10 specimens leading to initial values of K in the range of 31 MPa√m to 50 MPa√m and was equal to 12420 N and 10780 N for the two CT 20 specimens leading to initial values of K 29 MPa√m and 39 MPa√m. For the FLE 0.05 specimen, mean stress was equal to 312 MPa. In order to assess the influence of flaw position (CT 40-10 specimens), the six positions were tested under the following conditions : 600°C and K = 50 MPa√m. One specimen (numbered 1338-MB) sampled in the base metal plate was tested in the same conditions.

Most tests were interrupted before rupture, which was later obtained by room temperature fatigue.

EXPERIMENTAL RESULTS

Microstructural approach

A visual examination of the broken specimens shows that the creep crack front is not linear and that crack growth occurs preferentially at the center of the specimen (CT specimens) : figure 2. The scanning electron microscope observations of figure 3 show that rupture is intergranular in the base metal and interdendritic in the weld metal. Similar observations made on specimens with an initial flaw parallel to the welded joint lead to the same conclusion. Sections of the specimens were realised for microscopic observation after etching in order to determine crack path and localise damage. When the initial flaw is parallel to the welded joint, the crack tends to propagate inside the weld metal, along the fusion line. When the flaw is situated in the HAZ, the crack deviates towards the weld metal. When the flaw is perpendicular to the welded joint, the crack crosses the weld metal by propagating along interdendritic zones (as shown on figure 3), preferably along ferrite-austenite interfaces.

Whatever the flaw position, secondary cracks are observed within one millimeter of the rupture surface. Their number and length increase with test duration, which is typical of creep damage. Secondary cracks are mainly observed in the weld metal. Figure 4 represents a longitudinal section of specimen 4B : the weld metal is considerably more damaged than the base metal where onlyone short secondary crack is observed. Whatever the orientation of the initial flaw (perpendicular or parallel to the welded joint), damage and rupture are mainly localised in the weld metal, along the fusion line.

Global fracture mechanics approach

A displacement versus time curve was obtained for every test from the recording of the extensometer. By an initial calibration [1], the potential value measured across the crack, is correlated to the crack length to obtain a crack length versus time curve. An example is given in figure 5 (specimen 4B) : the differents zones through which the crack (initially perpendicular to the joint) propagated are indicated. Initiation time t_i is mentionned.

For a global fracture mechanics approach, parameter C^*_{ex}, which is an estimation of C* using experimental measurements, including $d\Delta/dt$, was determined.

For a CT specimen, Bensussan and al. [2] have developped the following expression, using the work of Harper and Ellison [3]

$$C^*_{ex} = \frac{n_2}{n_2+1} \cdot \frac{P\dot{\Delta}}{B(W-a)} \cdot A(a/W, n_2) \simeq 2 \cdot \frac{P\dot{\Delta}}{B(W-a)}$$ in the case of austenitic stainless steel

The experimental value of Δ depends upon the creep of the specimen and upon creep crack growth. The estimation of C* by C^*_{ex} is hence only valid for a stationnary crack, particularly at initiation time. C^*_{ex} is considered here as a mechanical parameter taking into account specimen geometry and loading, for C^*_{ex} is an estimation of C* only when secondary creep is predominant in the specimen. However the calculation of transition time t_1 and t_2 has shown that primary creep is predominant during the tests [4] (the tests are interrupted before rupture). But the parameter C^*_h, which represents the stress and strain fields in a situation of predominant primary creep can be estimated from C^*_{ex} by [2] :

$$C^*_h = (p1 + 1)\, t^{[p1/(p1+1)]}\, C^*_{ex}$$

For the axisymetric specimen, C*ex was calculated according to the formula : $C^*_{ex} = P\dot{\delta}/2\pi R^2$ [5], R being the radius of the notched section. The above mentionned remarks and limitations also apply to this formula. Figure 6 represents in logarithmic coordinates, time to initiation t_i and C^*_{ex} at crack initiation. The scatter band obtained by Bensussan and al. [2] for the base metal is drawn on the diagram.

The results corresponding to the CT 40 specimens are all inside this scatter band. The results corresponding to the CT 20 specimens are on the lower side of it or out of it. The result corresponding to the FLE 0.05 is out of it.

By linear regression, the following relation was obtained by taking into consideration only the results obtained on CT 40 specimens : $t_i\, C^*_{ex}{}^{0.78}$ = constant. The correlation coefficient is 0.94. If all results are included in the linear regression, the following relation is obtained : $t_i\, C^{*0.69}$ = constant. The diversity of specimen geometries here reduces the correlation coefficient which dwindles to 0.87.

DISCUSSION

If one takes into consideration CT 40 specimens only, by the global rupture mechanics approach one does not distinguish any difference between base metal and the composite specimen comprising weld metal and base metal. This is true whatever the initial flaw position among the six positions which were tested. However, the microscopic observations mentionned in 2.1 indicate that creep damage is preferentially localised in the weld metal along the fusion line. This seeming paradox is due to the fact that a CT 40 contains only 7 % weld metal, and the behaviour of the specimen is largely dependent upon the behaviour of the base metal. However, for the CT 20 specimens and the axisymetric specimen the proportion of weld metal (especially in high stress zones) is more important and its higher susceptibility to creep damage influences the macroscopic mechanical results. The above remarks indicate that from a safety point of view initiation criteria that would be developped from date obtained on specimens made wholly of weld metal would be conservative for a real structure which contains generally a large proportion of base metal.

CONCLUSIONS

The correlation between t_i and C^*_{ex} obtained on specimens containing 7 % weld metal is the same as the one obtained on base metal. In composite specimens containing both weld and base metal, creep damage and crack propagation tend to localise in the weld metal, close to the fusion line. The macroscopic behaviour of the specimen depends upon the proportion of weld metal present in the specimen. The data obtained on weld metal alone are not representative of the behaviour of composite structures but give conservative initiation rules for real components.

ACKNOWLEDGEMENTS

We wish to thank for their financial support of the study :
- NOVATOME
- Service Central de Sureté des Installations Nucléaires.

BIBLIOGRAPHICAL REFERENCES

[1] Patricia FESNEAU-FALBRIARD - Thèse soutenue le 6 Octobre 1987 - UTC Compiègne

[2] P. BENSUSSAN, R. PIQUES, A. PINEAU, ASTM 3rd Int. Symp. on Non-Linear Fract. Mech. Knoxville (USA), Oct. 1986

[3] M.P. HARPER, E.G. ELLISON, Jal. of Strain Anal., Vol. 12, n° 3, pp. 167-179, 1977

[4] P. FESNEAU-FALBRIARD, P. BALLADON, C. ESCARAVAGE, Proceedings of MECAMAT, Dourdan (France), 14-15 Oct. 1987

[5] R. PIQUES - Private communication

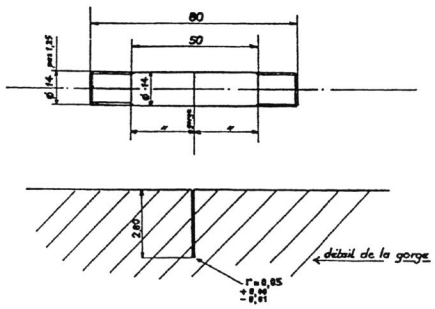

Fig. 1. Notched axisymetric specimen FLE 0.05

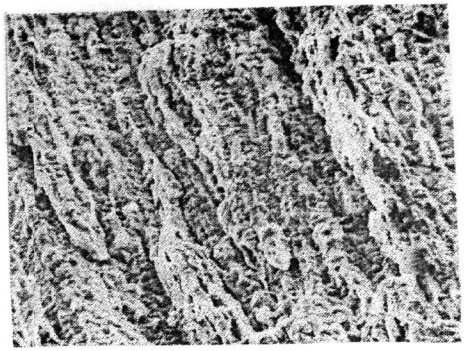

x 310

Fig. 3a. Interdendritic creep rupture in weld metal

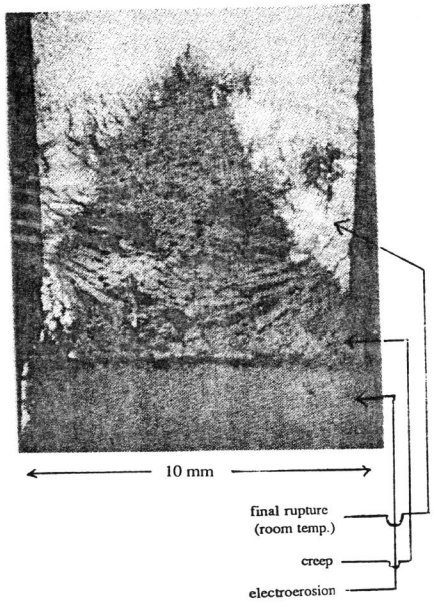

Fig. 2. Creep crack propagation
on a CT 40/10 specimen

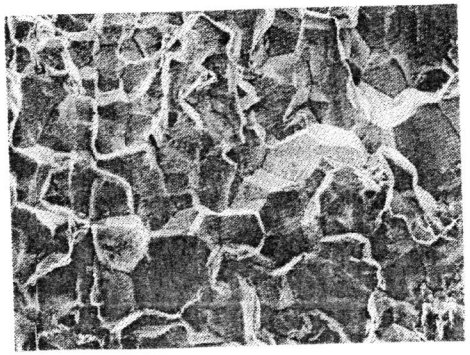

x 278

Fig. 3b. Intergranular creep rupture in parent metal

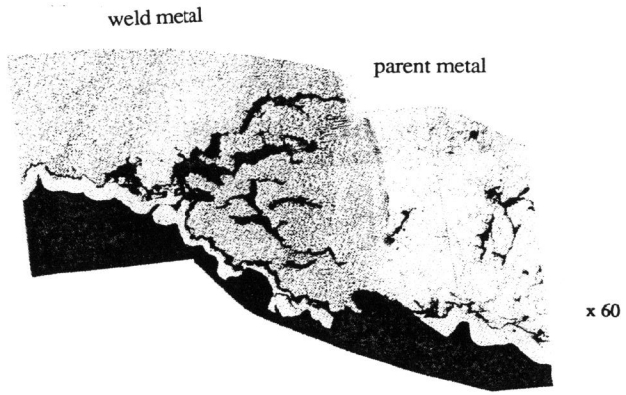

Fig. 4. Crack propagation and creep damage in specimen 4B

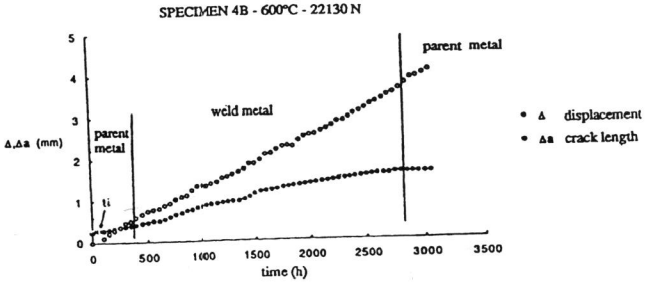

Fig. 5. Δ and a as functions of time (specimen 4B)

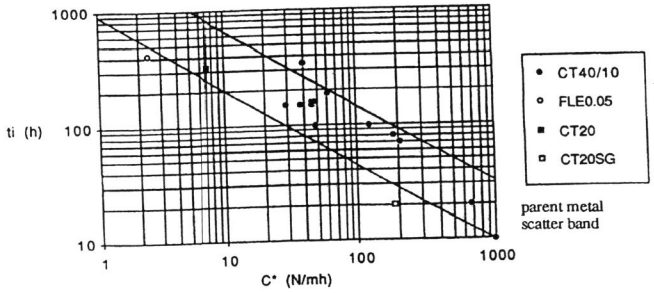

Fig. 6. ti-C* correlation